

Intermediate age open clusters: Collinder 110

Angela Bragaglia, Monica Tosi

INAF–Osservatorio Astronomico di Bologna, Via Ranzani 1, I-40127 Bologna, Italy, e-mail angela@bo.astro.it, tosi@bo.astro.it

ABSTRACT

We present CCD BV photometry of the intermediate age open cluster Collinder 110, a nearby, scarcely populated, and poorly studied system. There is no literature information on the metallicity, so we tested several possibilities, and found a slight evidence of sub-solar abundances. Using the synthetic Colour - Magnitude Diagrams technique we estimate the following parameters: age between 1.1 and 1.5 Gyr, reddening $0.38 \leq E(B - V) \leq 0.45$, distance modulus $(m - M)_0$ between 11.8 and 11.9 if the cluster metallicity is solar, or age between 1.2 and 1.7 Gyr, reddening $0.52 \leq E(B - V) \leq 0.57$, distance modulus $(m - M)_0$ between 11.45 and 11.7 if the cluster metallicity is sub-solar.

Key words: Hertzsprung-Russell (HR) diagram – open clusters and associations: general – open clusters and associations: individual: Collinder 110

1 INTRODUCTION

Open clusters are commonly believed to be excellent tracers of the Galactic disc properties. They can be observed in the whole disc, their parameters (e.g. distance, age, and metallicity) can be determined with an accuracy unreachable for other disc objects except the nearest ones, their ages cover the whole interval from a few million years to about 10 Gyr, so they can be used to study both the present day disc structure and its temporal evolution (Janes & Phelps 1994, Friel 1995, Tosi 2000, Bragaglia et al. 2002). In particular, intermediate age and old open clusters (i.e., with ages older than the Hyades) offer the best opportunity to trace the whole kinematical and chemical history of our disc, once granted the existence of populous and representative samples, accurately and homogeneously analysed (for recent works see e.g., Twarog, Ashman, & Anthony-Twarog 1997; Carraro, Ng, & Portinari 1998).

We are presently trying to build such a sample and to this end we have collected data over several years. We have already analysed in a homogeneous way eight clusters (see Di Fabrizio et al. 2001, and references therein). This paper is part of our general project, and is devoted to Collinder 110 (Cr 110, C 0635+020), a poorly populated, intermediate age open cluster located at $RA(2000) = 06:38:35$, $DEC(2000) = +02:02:27$, or $l = 209.66$, $b = -1.99$.

Cr 110 was previously studied by Dawson and Ianna (1998, hereafter DI98), who presented photographic and photoelectric measurements, and also reported results of an older paper by Tsarevskii & Abakumov (1971). They estimated $E(B - V) = 0.50 \pm 0.03$, distance 1950 ± 300 pc, and age of 1.4 ± 0.3 Gyr assuming solar abundance. Dutra and Bica (2000) cite a larger reddening ($E(B - V) = 1.12$) based on the Schlegel, Finkbeiner & Davis (1998) maps,

which however should be used with great caution at such low galactic latitudes (see e.g., Appendix C of Schlegel et al., where they suggest not to trust their predicted reddenings for $|b| < 5^\circ$).

We describe our data in Section 2, and the resulting colour - magnitude diagrams in Section 3. Section 4 is devoted to the derivation of the cluster parameters, while summary and conclusions are presented in Section 5.

2 OBSERVATIONS AND DATA REDUCTION

Cr 110 was observed with DFOSC (Danish Faint Object Spectrograph and Camera) at the 1.54m Danish telescope located in La Silla, Chile, on UT January 5 and 6, 1999. DFOSC was equipped with CCD #C1W7 (Loral/Lesser, $2k \times 2k$ pixel, $0.4''/\text{pixel}$, field of view of 13.7 arcmin^2), and the Johnson standard system filters. The two nights appeared photometric; seeing values varied between about $1.5''$ and $1.8''$. We obtained 6 exposures in the B filter (10, 20, 60, 120, 360, 600 s) and 5 in the V filter (5, 20, 60, 180, 300 s) on a field centered on the cluster, and 2 exposures in B and V on a second, partly overlapping field (20 and 240 s, 10 and 120 s in the two bands respectively) we observed to account for field stars contamination. Fig. 1 shows our fields, and the DI98 one.

All frames were trimmed and corrected for bias and flat fields in the standard way, using IRAF¹ tasks. We then used DAOPHOT-II, also in IRAF environment, to find and measure stars (Stetson 1987, Davis 1994). All frames were

¹ IRAF is distributed by the NOAO, which are operated by AURA, under contract with NSF

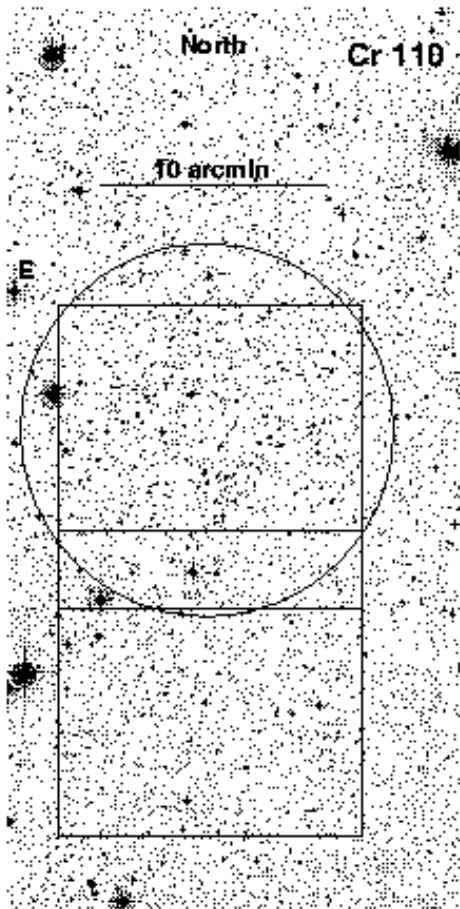


Figure 1. Map of our field (the central square) of 13.5 arcmin^2 ; also shown is a second field used for field stars comparison, and the zone observed by Dawson & Ianna (1998, fig. 1, the circle).

searched independently, using the appropriate value for the FWHM of the stellar profile and a threshold of 4σ over the local sky value. About 30 well isolated, bright stars distributed all over the frame were used in each image to define the best analytical PSF model (we used a gaussian with spatial variations), which was then applied to all detected objects. The resulting magnitude file was selected in magnitude, to avoid saturated stars, in error (only stars with $\sigma \leq 0.1$ were retained, and almost all rejections were in the lower magnitude bins), in goodness-of-fit estimator ($\chi^2 \leq 2$), and in shape - defining parameter ($-1 \leq \text{sharpness} \leq 1$), to avoid cosmic rays and false identifications of extended objects. Fig. 2 shows the distribution in error, χ^2 , and *sharpness* for the reference *B* and *V* frames, with lines indicating our selection criteria.

We computed a correction to the PSF derived magnitudes to be on the same system as the photometric standard stars: aperture photometry was performed on a few isolated stars (the same used to define the PSF) in the reference image for each filter. The corrections (in the sense aperture

minus PSF) were found to be -0.187 in *B*, and -0.223 mag in *V*.

All output catalogues referring to the central field were aligned to the one derived from the reference *B* image, assumed as master frame for the coordinate system, using dedicated programs developed at the Bologna Observatory by P. Montegriffo. We then "forced" the output catalogues in both filters to the reference ones applying linear transformations (almost zero point shifts) to the instrumental magnitude. The final magnitudes in each band are the result of the average of all measures for each star.

Equatorial coordinates for all stars in the final catalogue were computed using another dedicated program developed by P. Montegriffo, which cross correlates positions (in pixel) of our stars with positions (in RA and DEC) of objects in the second edition of the Guide Star Catalogue,² and computes suitable transformations. The r.m.s. of the transformation was of about $0.1''$ in both coordinates.

The external field was also aligned in magnitude to the *B* and *V* reference central fields, using stars in common, and formed a separate catalogue.

2.1 Photometric calibration

The conversion of the final, averaged catalogue from instrumental magnitudes to the Johnson standard system was obtained using the standard area PG0231+051 (Landolt 1992) observed four times just before and after the cluster on the first night. The standards span a fairly wide range in colour ($-0.329 \leq B - V \leq 1.448$), adequate for the cluster stars. Aperture photometry was used to measure their magnitudes.

Extinction coefficients were derived from the standard stars, since they were observed at different airmasses: $\kappa_V = 0.1354$ and $\kappa_B = 0.2287$ (Clementini, private communication). No second order extinction coefficients were estimated, but they are usually close to zero, and can safely be ignored if one does not aim to milli-mag accuracy (intrinsically impossible with the instrument we used, which is not designed for very high precision photometry). Moreover our data were not acquired at large airmasses so there is no strong need of a color-dependent extinction correction, which accounts for differential absorption at the blue and red ends of the filter passbands. The extinction coefficients used in this work compare well to the average values for the site ($\kappa_V \simeq 0.12$, $\kappa_B \simeq 0.22$) and to the ones derived for another night of the same run (UT January 7 1999) using different objects i.e., stars in the Large Magellanic Cloud observed the whole night at very different airmasses ($\kappa_V = 0.114$, $\kappa_B = 0.252$, Clementini, private communication).

The instrumental magnitudes of the standard stars were corrected for extinction and to an exposure time of 1 second, and from comparison to the tabulated value we derived the following calibration:

$$B = b + 0.0999 \times (b - v) - 1.0633 \quad (r.m.s. = 0.0114)$$

² The Guide Star Catalogue-II is a joint project of the Space Telescope Science Institute and the Osservatorio Astronomico di Torino

Table 1. Completeness ratios in the two bands.

mag	compl B	compl V
<15.5	1.00	1.00
15.50	0.99	0.99
15.75	0.97	0.95
16.00	0.98	0.97
16.25	0.96	0.95
16.50	0.96	0.95
16.75	0.96	0.95
17.00	0.96	0.94
17.25	0.96	0.94
17.50	0.93	0.93
17.75	0.94	0.92
18.00	0.96	0.94
18.25	0.95	0.92
18.50	0.93	0.93
18.75	0.93	0.92
19.00	0.94	0.90
19.25	0.93	0.93
19.50	0.94	0.93
19.75	0.94	0.90
20.00	0.90	0.89
20.25	0.92	0.92
20.50	0.92	0.84
20.75	0.89	0.83
21.00	0.87	0.78
21.25	0.82	0.51
21.50	0.69	0.08
21.75	0.35	0.00
22.00	0.04	
22.25	0.00	

$$V = v + 0.0063 \times (b - v) - 0.6075 \quad (r.m.s. = 0.0163).$$

These equations, where B and V are the Johnson magnitudes, and b and v are the instrumental magnitudes, corrected for aperture, exposure time and extinction, were then used to build our final photometric catalogue.

DI98 presented also photoelectric measurements, and we compared the B and V values for the about 30 stars in common. We noticed a small trend, i.e., our magnitudes are brighter than the photoelectric ones at the bright end, and fainter at the faint end, but with a large scatter. We have derived a correction and applied it to our catalogue; however, when comparing our corrected Colour - Magnitude diagram with the photographic one by DI98, calibrated using the photoelectric measures, not only we did not find any clear improvement, but a worsening was possible. We then decided not to apply any correction.

2.2 Completeness analysis

We tested the completeness of our stellar detections on the deepest B and V images, adding artificial stars to each frame and exactly repeating the procedure of extraction of objects and PSF fitting used for the original frame. The stars were added at random positions and selected in magnitude according to the observed luminosity function. We added only 960 objects at a time, and the process was repeated as many times as to reach a total of about 50,000 artificial stars. In

fact, in order not to significantly alter the crowding conditions we added each object in a 60×60 pixel box, excluding the image borders. This way we approximate the condition of adding a single star each time, i.e. of a repeated, independent experiment, since the artificial objects added in a single run do not interfere with each other. To the output catalogue of the added stars we applied the same selection criteria in magnitude, error, χ^2 and sharpness as done for the science frames. The completeness degree of our photometry at each magnitude level was computed as the ratio of the number of recovered artificial stars to the number of added ones, and is given in Table 1.

The difference between input and output magnitudes of the artificial stars provide an estimate of the photometric error alternative to the Daophot σ . The average value associated to each magnitude bin is smaller than the corresponding σ 's, as expected when errors do not come from blends due to very crowded conditions, so we adopted the Daophot σ 's for the synthetic CMDs (see Section 4).

3 THE COLOUR - MAGNITUDE DIAGRAM

The final, calibrated sample consists of 1854 stars for which at least one B and one V measures were obtained; as already said in the previous Section, whenever more than one value was available we adopted the average (after σ clipping) of all measurements. The table with B and V magnitudes and equatorial coordinates is available through the BDA (Mermilliod 1995: obswww.unige.ch/webda/). The corresponding colour - magnitude diagram (CMD) is shown in Fig. 3(b), and can be compared with the DI98 one of Fig. 3(a).

The Turn-Off point from the main sequence (MSTO) is located at $V \simeq 15.25$, and $B - V \simeq 0.64$, and a red clump (the core He burning phase) is well visible, at $V \simeq 13.6$ and $B - V \simeq 1.33$. That this second feature is attributable to the cluster appears clear when looking at the external comparison field (Fig. 3(c)) where no clump stars (or very few, as expected since there is some overlap) are visible.

The cluster MS is well defined, but embedded in a fairly large strip due to the fact that the cluster is strongly contaminated by field stars. Since we also have a second pointing not centered on the cluster, we could try to statistically subtract field stars and isolate the cluster sequences. This was done, but results were not satisfactory, given the small numbers involved and the fact that the second field is still too close to the cluster centre and probably contains some members. We then tried another approach, and divided the central field in nine boxes of about 700×700 pixels, plotting separately the CMD's for each zone (Fig. 4). As it can be seen, the cluster main sequence stands clearly over the field component only in the very central zone: we decided to consider only stars falling in this reduced field as *bona fide* cluster members, to be compared with theoretical synthetic populations.

DI98 also determined proper motions for about 60 % of stars with $V, B - V$ data (their tab.5), but no clear separation between cluster and field stars is visible from their data (their fig.2). They label as field stars those with proper motions in either coordinate larger than 1.2 arcsec per century, but this criterium is not stringent enough: it excludes only about 10 % of the sample, without any improvement in

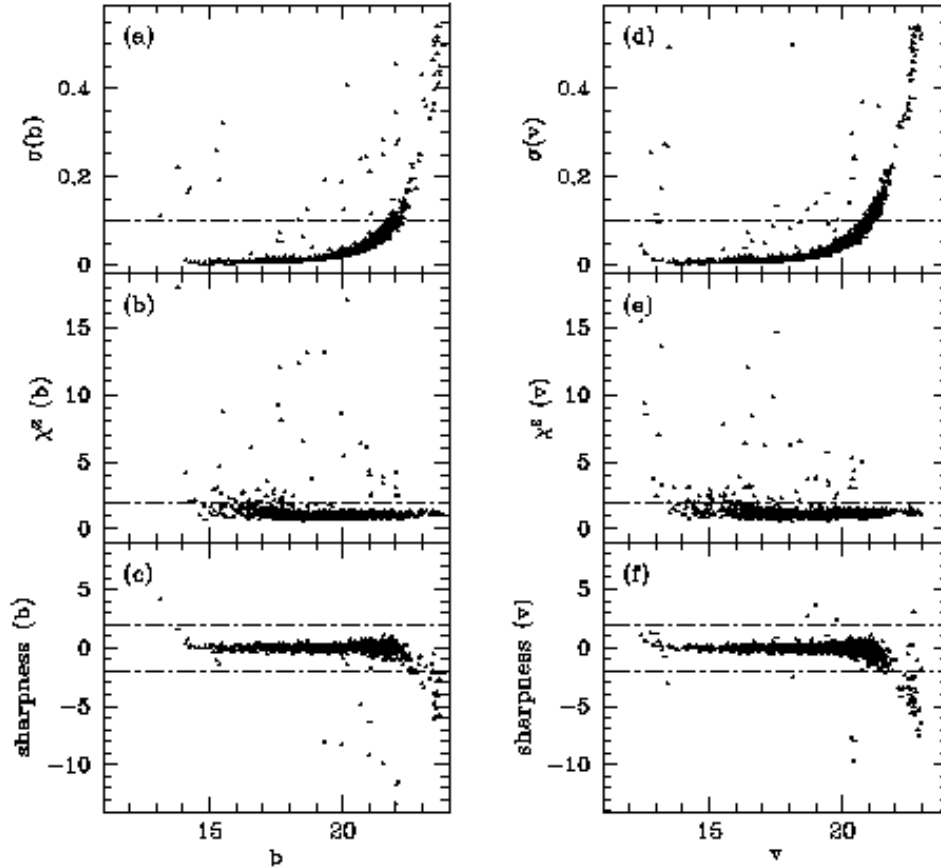


Figure 2. Distribution of errors (the DAOPHOT σ), χ^2 , and *sharpness* for the B and V reference frames. Note that we plot the instrumental b and v magnitudes.

the CMD. We then decided to disregard the proper motion information in the following.

4 CLUSTER PARAMETERS

In order to derive the age, distance and reddening of Cr 110, we have applied the synthetic CMD method (Tosi et al. 1991) already used and described for the other clusters of our sample. We have adopted as reference observational CMD that of the central box of Fig. 4, which contains 260 stars. The synthetic CMDs therefore contain 260 stars extracted with a MonteCarlo procedure from the adopted sets of stellar evolution tracks. The synthetic stars are affected by the same photometric errors as the actual data and selected according to the completeness factors listed in Section 2.2 (Table 1). The transformations from the theoretical luminosity and effective temperature to the Johnson magnitudes and colours have been performed using Bessel, Castelli & Pletz (1998) conversion tables.

We have amply demonstrated in the past that the derived parameter values depend on the adopted stellar evolu-

tion models. Hence, to give an estimate of the corresponding uncertainties, one should always derive them assuming various sets of stellar models computed with different assumptions. For Cr 110 we have adopted homogeneous sets of stellar tracks computed by three different groups: i) the Padova models (hereinafter BBC, Bressan et al. 1993, Fagotto et al. 1994), which take into account the effect of overshooting from convective regions, ii) the FST tracks (Ventura, D’Antona & Mazzitelli 2003 in preparation), with various amounts of overshooting, and iii) the FRANEC tracks (hereinafter FRA, Dominguez et al. 1999), computed without overshooting. Since the metallicity of Cr 110 is unknown, for all these sets we have considered both solar and sub-solar initial compositions. In practice we have simulated the observed CMDs adopting the stellar models listed in Table 2.

All the synthetic CMDs have been computed either assuming that all the cluster stars are single objects or that a fraction of them are members of binary systems. The data on Cr 110 don’t allow to safely infer such fraction, but we find that one around 20% seems to better reproduce the ob-

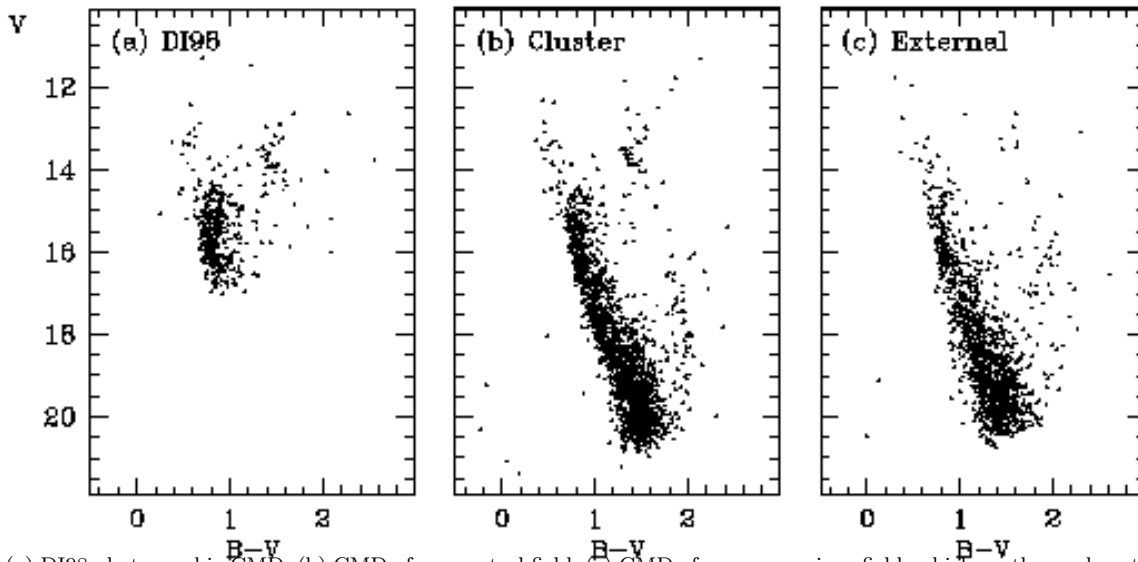


Figure 3. (a) DI98 photographic CMD; (b) CMD of our central field; (c) CMD of our comparison field, which partly overlaps the central one

Table 2. Stellar evolution models adopted for the synthetic CMDs

Set	metallicity	overshooting	Reference
BBC	0.02	yes	Bressan et al. 1993
BBC	0.008	yes	Fagotto et al. 1994
BBC	0.004	yes	Fagotto et al. 1994
FRA	0.02	no	Dominguez et al. 1999
FRA	0.01	no	Dominguez et al. 1999
FRA	0.006	no	Dominguez et al. 1999
FST	0.02	$\eta=0.02$	Ventura et al. in prep.
FST	0.02	$\eta=0.03$	Ventura et al. in prep.
FST	0.006	$\eta=0.02$	Ventura et al. in prep.
FST	0.006	$\eta=0.03$	Ventura et al. in prep.

served distribution and spread of the cluster main sequence. Indeed, despite the uncertainties, models with lower binary fractions lead to excessively tight MSs, while models with 30% begin to show a MS spread larger than observed. All the CMDs shown in the figures assume that 20% of the stars are binaries with random mass ratios.

The relatively low number of stars measured in this cluster, especially in key regions of the CMD such as the MSTO, the clump and the red giant branch (RGB), in principle could not let us firmly discriminate between similar synthetic cases. Furthermore, the empirical luminosity function (LF) of the 260 supposed cluster members may be somewhat contaminated by background objects, especially at its faint end, which adds another uncertainty to the selection. Nonetheless, the shape and the number of stars present in the key evolutionary phases, as well as the magnitude and colour difference between MSTO and clump, allow to derive

a quite restricted range of possible ages for each adopted set of tracks. Moreover, the stable results obtained for each assumed metallicity on distance modulus and reddening allow us to reach firm conclusions on these values too.

Fig. 5 shows the best cases of synthetic CMDs (top) and LFs (bottom) resulting from solar metallicity tracks. The left hand panels refer to the case with BBC tracks, age=1.35 Gyr, $E(B-V)=0.40$ and $(m-M)_0=11.8$, the central ones to the case with FRA tracks, age=1.1 Gyr, $E(B-V)=0.45$ and $(m-M)_0=11.9$, and the right hand panels to the case with the FST tracks ($\eta=0.02$), age=1.5 Gyr, $E(B-V)=0.38$ and $(m-M)_0=11.8$.

All the models with solar metallicity need to assume a reddening systematically lower than the literature value ($E(B-V)=0.5^3$) to reproduce the observed colours. $E(B-V)=0.45$ is the maximum acceptable value, but 0.38–0.40 is more frequently found. As a consequence, the resulting distance modulus is systematically larger than that derived by DI98 ($(m-M)_0=11.45$), and never shorter than $(m-M)_0=11.6$. Vice versa, models with sub-solar metallicity allow for larger reddenings and for distance moduli in agreement with that by DI98.

Fig. 6 shows representative cases of synthetic CMDs (top) and LFs (bottom) resulting from stellar models with initial metallicity lower than solar and in better agreement with the data. The left hand panels refer to the case with BBC tracks with $Z=0.004$, age=1.7 Gyr, $E(B-V)=0.57$ and $(m-M)_0=11.45$, the central ones to the case with FRA tracks with $Z=0.01$, age=1.2 Gyr, $E(B-V)=0.52$ and $(m-M)_0=11.7$, and the right hand panels to the case with the

³ Actually, DI98 derived $E(B-V)=0.53$ from the UBV two colours diagram for 22 probable cluster members, while 0.50 is the value derived from isochrone fitting.

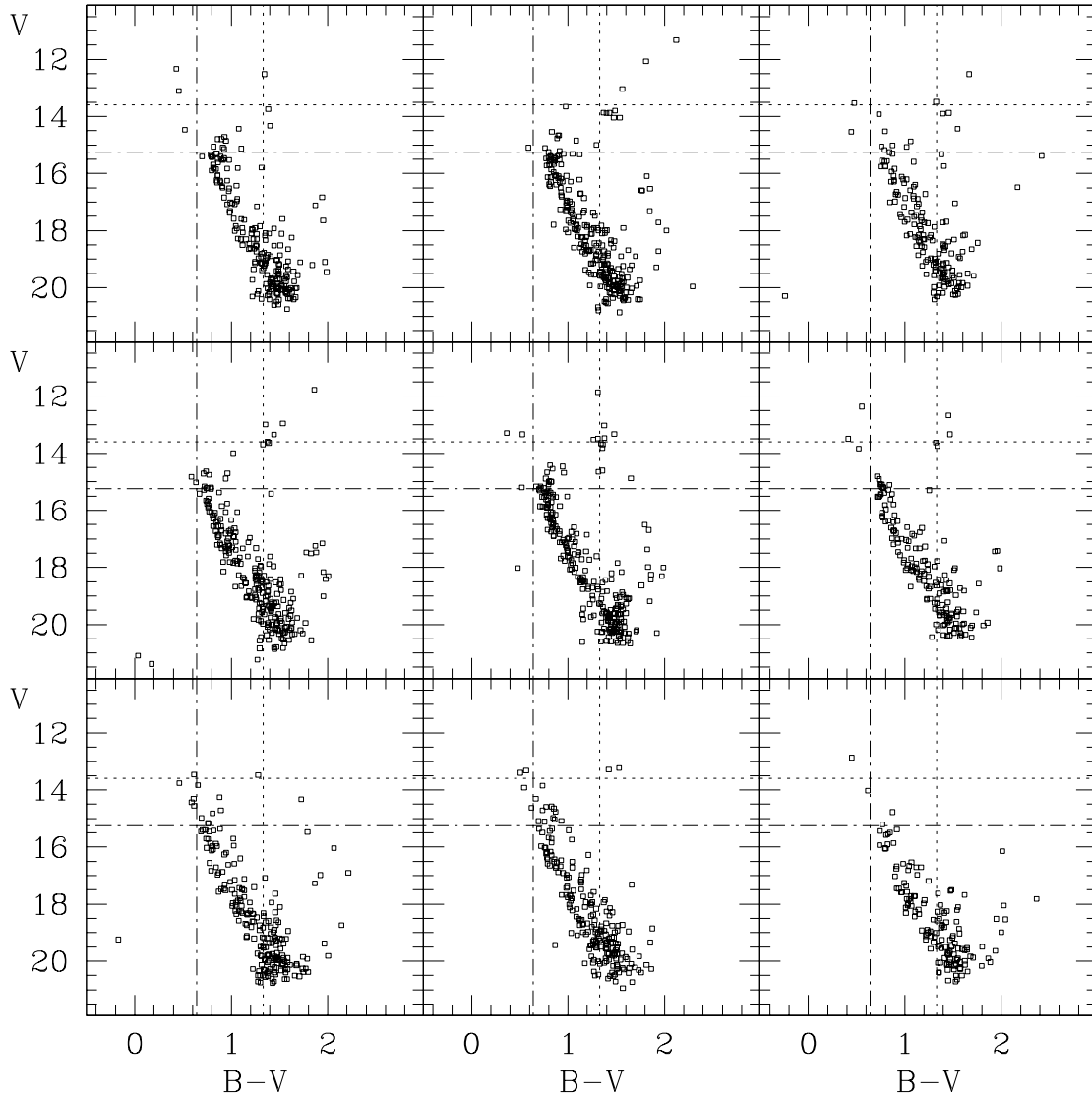


Figure 4. The central field has been divided in a grid of nine 700×700 pixels zones, and a CMD is plotted for each of them. The lines are drawn to help identify the TO and clump positions. Notice how the field contamination is negligible only in the very central panel.

FST tracks ($\eta=0.02$) with $Z=0.006$, age=1.5 Gyr, $E(B - V) = 0.56$ and $(m-M)_0=11.45$.

The main difference between the values we obtain with different stellar models is the consequence of the different treatments of the convective zones. Indeed, as well known, the age resulting from stellar models is increasingly older for increasing amount of assumed overshooting, due to the fact that larger cores make the model star brighter. In turn, for a given metallicity, older ages correspond to predicted redder intrinsic MSTO colours, and therefore need lower $E(B - V)$ to reproduce the observed colour.

In general, we find that a better agreement with the observed cluster features is obtained when assuming a metallicity lower than solar. The shape and the stellar distribution in the CMD of MS, MSTO, clump and RGB as well as the LFs are all better reproduced by low metallicity models. How much lower than solar is difficult to say, because the formal metallicity of the stellar tracks is actually a combination of chemical composition, opacities, etc., and therefore its ef-

fect may vary from one set to another. In fact, we find that, when adopting the BBC models, $Z=0.004$ provides better results than $Z=0.008$, while with the FRA models $Z=0.01$ looks better than $Z=0.006$, but $Z=0.006$ is fine with the FST models. These apparent inconsistencies are simply the proof that photometric use of stellar models alone is not a good metallicity indicator; at most it can be useful to infer a metallicity ranking. No doubt that spectroscopic observations of Cr 110 are needed to safely derive its true chemical abundance and restrict the choices for the other cluster parameters.

5 SUMMARY AND CONCLUSIONS

Cr 110 is a fairly poor cluster, highly contaminated by background objects, with the further disadvantage that the latter have a distribution in the CMD not too different from that of the cluster members, a circumstance that makes separa-

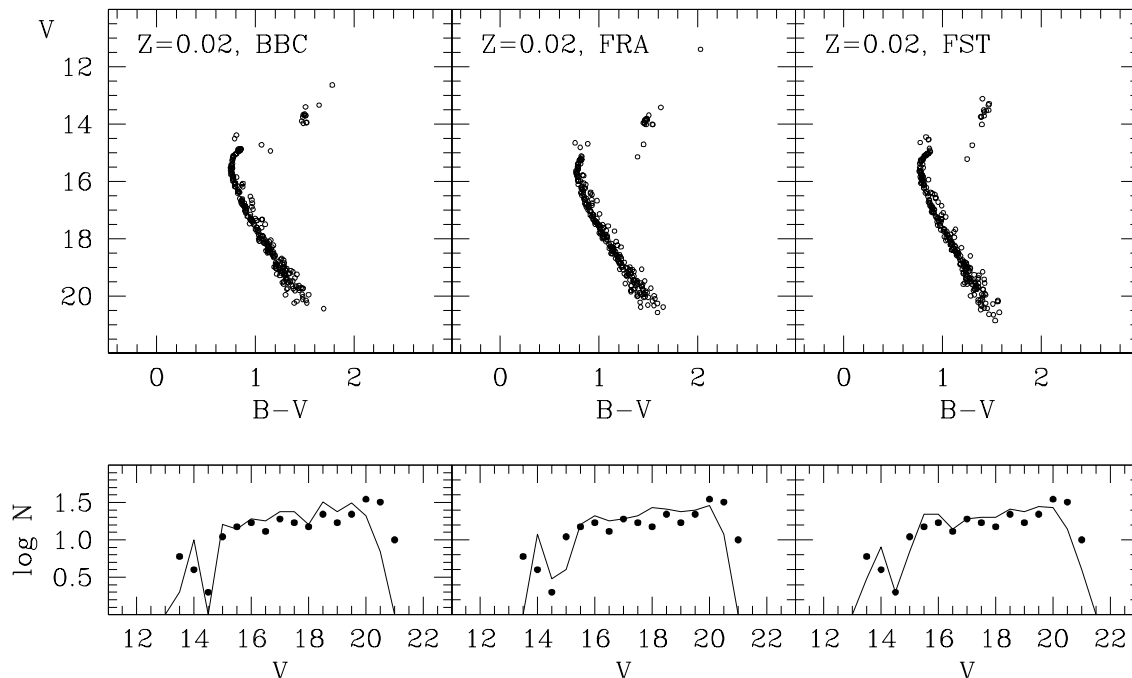


Figure 5. Synthetic CMDs (top) and LFs (lines in the bottom panels) resulting from solar metallicity models. The dots in the bottom panels show the empirical LF of the 260 stars in the CMD of the central panel of Fig. 4. The displayed cases are: BBC models assuming age=1.35 Gyr, $E(B - V) = 0.40$, $(m-M)_0 = 11.8$, on the left; FRA models assuming age=1.1 Gyr, $E(B - V) = 0.45$, $(m-M)_0 = 11.9$, on the center, and FST models with $\eta = 0.02$ assuming age=1.5 Gyr, $E(B - V) = 0.38$, $(m-M)_0 = 11.8$, on the right.

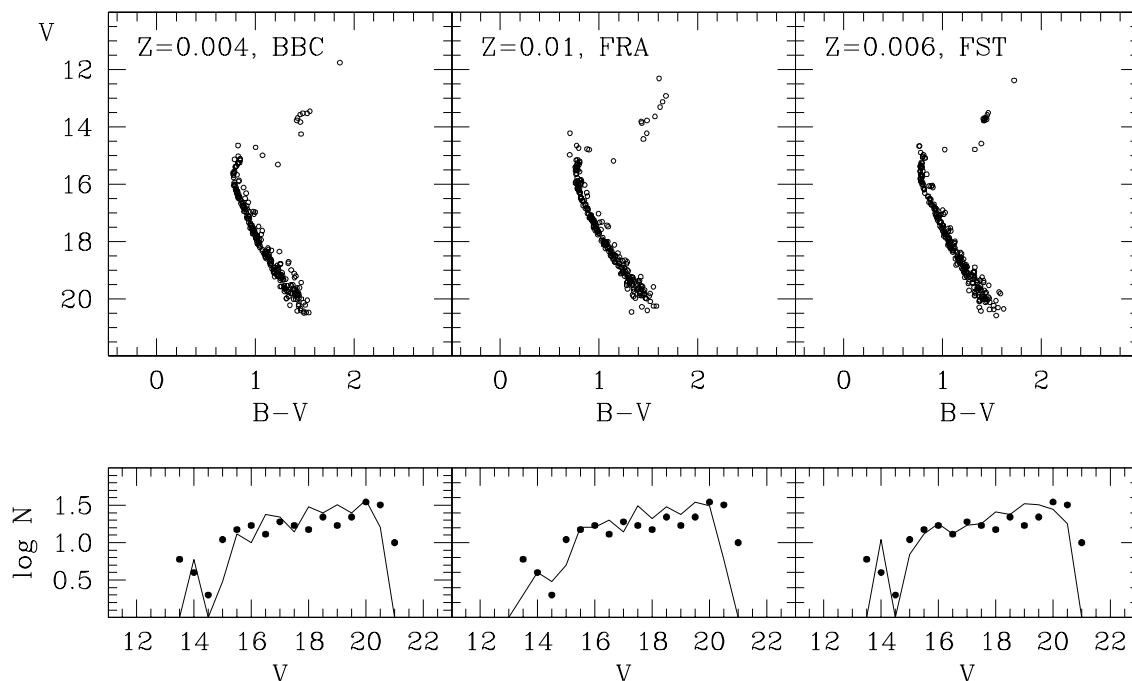


Figure 6. Synthetic CMDs (top) and LFs (lines in the bottom panels) resulting from models with initial metallicity lower than solar. The dots in the bottom panels show the empirical LF of the stars in the CMD of the central panel of Fig. 4. The displayed cases are: BBC tracks with $Z = 0.004$, age=1.7 Gyr, $E(B - V) = 0.57$ and $(m-M)_0 = 11.45$, on the left; FRA models assuming $Z = 0.01$, age=1.2 Gyr, $E(B - V) = 0.52$ and $(m-M)_0 = 11.7$, on the center, and FST models assuming $\eta = 0.02$, $Z = 0.006$, age=1.5 Gyr, $E(B - V) = 0.56$ and $(m-M)_0 = 11.45$, on the right.

tion of true cluster members particularly uncertain. In spite of that, we are able to attribute to Cr 110 fairly restricted ranges of age, reddening and distance modulus, whose uncertainty is mostly related to the different possible theoretical approaches and to the unknown metallicity. If the cluster metallicity is solar, its age ranges between 1.1 Gyr (based on stellar models with no overshooting) and 1.5 Gyr (based on models with a large amount of overshooting), the reddening is $E(B - V)$ around 0.4 and the distance modulus larger than 11.6. If the metallicity is less than solar, the age ranges between 1.2 Gyr (no overshooting) and 1.7 Gyr (overshooting), the reddening is between 0.52 and 0.58 and the distance modulus 11.45 or slightly larger.

We suggest that the cluster metallicity be lower than solar because the corresponding synthetic CMDs are more capable to reproduce the shape of the various evolutionary sequences, their number of populating stars and their relative colour and magnitude differences. In addition, with a metal poor chemical composition we obtain values for the reddening and the distance modulus in much better agreement with those derived by DI98. The metal poor synthetic CMDs in better agreement with the data assume in fact $0.52 \leq E(B - V) \leq 0.57$ and $11.45 \leq (m-M)_0 \leq 11.7$.

Better and more stringent constraints require further observations: spectroscopy at (at least) medium resolution of a large sample of objects to determine membership, and at high resolution of a few member stars to measure detailed chemical abundances. This way Cr 110 could appropriately take its place in our slowly growing sample of well studied open clusters.

ACKNOWLEDGEMENTS

This work is based on observations collected at the European Southern Observatory, Chile. We warmly thank P. Montegriffo, whose programs were used for the data analysis, and E. Sabbi for her expert advice. We also thank L. Di Fabrizio and G. Clementini for providing the standard stars photometry and the extinction coefficients, and F. D'Antona and P. Ventura for providing their unpublished stellar models. The bulk of the simulation code was originally provided by L. Greggio. Financial support to this project has come from the MURST-MIUR through Cofin98 "Stellar Evolution", and Cofin00 "Stellar Observables of Cosmological Relevance". This research has made use of the Simbad database, operated at CDS, Strasbourg, France. Finally we acknowledge the use of the valuable BDA database, maintained by J.-C. Mermilliod, Geneva.

REFERENCES

- Bessel, M.S., Castelli, F., Plez, B. 1998, *A&A*, 337, 321
 Bragaglia, A., Tosi, M., Marconi, G., Di, Fabrizio L. 2002, T. Lejeune, J. Fernandez eds, *Observed HR Diagrams and stellar evolution: the interplay between observational constraints and theory*, Coimbra, ASP Conf. Ser., in press
 Bressan, A., Fagotto, F., Bertelli, G., Chiosi, C. 1993, *A&AS*, 100, 647
 Carraro, G., Ng, Y.K., & Portinari, L. 1998, *MNRAS*, 296, 1045
 Davis, L.E. 1994, *A Reference Guide to the IRAF/DAOPHOT Package*, IRAF Programming Group, NOAO, Tucson
 Dawson, D.W., Ianna, P.A. 1998, *AJ*, 115, 1076 (DI98)
 Di Fabrizio, L., Bragaglia, A., Tosi, M., Marconi, G. 2001, *MNRAS*, 328, 795
 Dominguez, I., Chieffi, A., Limongi, M., Straniero, O. 1999, *ApJ*, 525, 226
 Dutra, C.M., Bica, E. 2000, *A&A*, 359, 347
 Fagotto, F., Bressan, A., Bertelli, G., Chiosi, C. 1994, *A&AS*, 105, 29
 Friel, E.D. 1995, *ARAA*, 33, 38
 Janes, K.A., Phelps, R.L. 1994, *AJ*, 108, 1773
 Landolt, A.U. 1992, *AJ*, 104, 340
 Mermilliod, J.C. 1995, D. Egret, M.A. Albrecht, eds, *Information and On-Line Data in Astronomy*, Kluwer Academic Press (Dordrecht), p. 127
 Schlegel, D.J., Finkbeiner, D.P., Davis, M. 1998, *ApJ*, 500, 525
 Stetson, P.B. 1987, *PASP* 99, 191
 Tosi, M. 2000, F. Matteucci, F. Giovannelli eds, *The chemical evolution of the Milky Way: Stars versus clusters*, Kluwer Academic Publishers (Dordrecht), 255, p. 505
 Tosi, M., Greggio, L., Marconi, G., Focardi, P. 1991, *AJ*, 102, 951
 Tsarevskii, G.S., & Abakumov, I.E. 1971, *Astron. Tsirk.*, 631, 6
 Twarog, B.A., Ashman, K.M., & Anthony-Twarog, B. 1997, *AJ*, 114, 2556